Electrons and positrons in the galactic cosmic rays

A. M. Atoyan
Yerevan Physics Institute, Yerevan, Armenia
and Max-Planck-Institut für Kernphysik, Heidelberg, Germany

F. A. Aharonian and H. J. Völk
Max-Planck-Institut für Kernphysik, Heidelberg, Germany

(Received 8 August 1994; revised manuscript received 4 April 1995)

The detection of primary cosmic ray electrons with energies above 1 TeV implies the existence of a nearby, $r \leq 100$ pc, and relatively young, $t \leq 10^5$ yr, source(s) of accelerated electrons. Therefore a correct treatment of the formation of the spectra of electrons during their propagation in the interstellar medium requires a separate consideration of the contribution of one (or a few) nearby source(s) from the contribution of distant ($R \geq 1$ kpc) sources. To implement this approach, the problem of energy-dependent diffusive propagation of relativistic particles from a single source is considered, and the analytical solution to the diffusion equation in the general case of arbitrary energy losses and injection spectrum of primary particles is found. We show that in the framework of the proposed two-component approach, i.e., separating the contribution of the local (discrete) source(s) from the contribution of distant sources, it is possible to explain all the locally observed features of the energy spectrum of cosmic ray electrons from sub-GeV to TeV energies. In addition, assuming that the local source produces electrons and positrons in equal amounts, the model allows us to explain also the reported increase of the positron content in the flux above 10 GeV.

PACS number(s): 98.70.Sa, 52.25.Dg, 97.60.Gb

I. INTRODUCTION

It is commonly believed that the energy spectrum of the electron component of cosmic rays (CR's) as is observed in the solar system, at least its energy spectrum above 1 GeV, can be explained in the framework of standard (leaky-box or diffusion) galactic CR propagation models (for reviews, see, e.g., [1,2]). However, the measured content of positrons in the total electron flux, $C_+ = e^+/(e^- + e^+)$, at least at high energies $E \geq 10$ GeV, is regarded as a possible "enigma" [3] awaiting an explanation. The key problem here is to explain the sharp increase of the fraction of positrons above 10 GeV, reaching values that exceed 10%. This is almost an order of magnitude larger than expected for the positrons produced in interactions of CR's with interstellar gas nuclei. Therefore it is obvious that some other source of positrons is needed. In the framework of standard CR propagation models, assuming continuous and homogeneous distribution of CR sources in the Galaxy, the sharp increase of C_+ above 10 GeV should be essentially associated with the production spectrum of high-energy positrons. In fact, a few models with a high-energy threshold of positron production have been suggested. Their disadvantage is that they invoke either hypothetical physical processes [e.g., annihilation of weakly interacting massive particles, (WIMP's) [4,5]] or special circumstances [e.g., production of (e^+, e^-) pairs near compact γ-ray sources by the γ rays interacting with optical-UV photons assumed to be produced in the same sources [6]], and therefore they are not generally accepted.

Actually, the severe constraint on the positron production spectrum may disappear when inhomogeneous (or single source) models are concerned. Moreover the validity of spatially homogeneous and temporally continuous source models is significantly limited for CR electrons, at least in the very high-energy region (e.g., see [7–10]). Indeed, the observed energy spectrum of CR electrons extends without indication of a cutoff up to $E \approx 2$ TeV [11]. The radiative (Compton and synchrotron) cooling time of 2-TeV electrons in the interstellar medium (ISM) is only about 10^5 yr. In combination with the conventional CR diffusion coefficient this limits the distances to sources to no more than several hundreds of parsecs [7,10]. Thus, the sources of TeV electrons are limited both in time and space: we see electrons produced recently, and in sources distributed in the local environment. Most probably there are only a few (if not indeed only one) discrete sources responsible for the flux observed. Therefore a *single-source* rather than a *continuously distributed multiple-source* approach should be applied to high-energy electrons. This statement does not exclude that the lower-energy electrons observed result from contributions of *many* distant sources.

In this paper we propose the following *two-component* model: (i) the bulk of electrons, consisting mainly of e^-, is produced in distant (> 1 kpc) sources, distributed more or less uniformly both in space and time in the Galaxy; (ii) in addition, there is one (or a few) nearby (at distances $r \sim 100$ pc) and relatively young ($t \leq 10^5$ yr) source(s) of very high-energy electrons with a spectrum that extends beyond 1 TeV.

The idea of separation of the contributions of distant and nearby sources to the total flux of high-energy electrons was discussed earlier by Shen [7], Shen and Mao [8], and Cowsik and Lee [9] (initially for CR protons and nuclei by Lingenfelter [12]). However, there are significant differences between our approach and the previous ones. The main difference is that in this paper we study the *energy-dependent* diffusive propagation of electrons from a nonstationary point source while earlier only the case of energy-independent diffusion was considered. We present the Green's function solution for the nonstationary equation of the *energy-dependent* diffusion of particles from a single source in the case of *arbitrary* injection spectrum and an *arbitrary* energy loss. The solution has a simple analytical form which allows one to analyze easily the case of diffusion of particles from sources distributed *in space* and *in time*.

We show that in the framework of the proposed two-component approach, consisting in separation of the contributions of the local source(s) from the contribution of distant sources (assumed to be continuously distributed in the Galactic disk), it is possible to explain all the locally observed features of the energy spectrum of cosmic ray electrons from sub-GeV to TeV energies. In addition, assuming that the local source is an accelerator of (e^+, e^-) pairs, the model allows one to explain also the possible increase of the positron content in the flux above 10 GeV reported independently by several groups.

II. PROPAGATION OF COSMIC RAYS FROM A SINGLE SOURCE

In the standard diffusion approximation (i.e., neglecting convection) the propagation of CR's is described by the familiar diffusion equation (e.g., see [13]) which in the spherically symmetric case reduces to the form

$$\frac{\partial f}{\partial t} = \frac{D}{r^2}\frac{\partial}{\partial r}r^2\frac{\partial f}{\partial r} + \frac{\partial}{\partial \gamma}(Pf) + Q. \tag{1}$$

Here $f(r,t,\gamma)$, with $\gamma = E/m_e c^2$, is the energy distribution function of particles at instant t and distance r from the source; $P(\gamma) = -d\gamma/dt$ is the continuous energy loss rate; and D denotes the energy-dependent diffusion coefficient $D(\gamma)$. We have assumed D to be independent of r, i.e., a homogeneously diffusive medium is supposed. The Green's function $G(r,t,\gamma)$, i.e., the solution of Eq. (1) for a δ-function-type injection rate of monoenergetic particles $Q(r,t,\gamma) \propto \delta(\mathbf{r})\delta(t-t_0)\delta(\gamma-\gamma_0)$, is known [13,14]. For an arbitrary injection spectrum $Q \propto \Delta N(\gamma)$ the solution of Eq. (1) can be obtained by convolution of $\Delta N(\gamma)$ with $G(r,t,\gamma)$. However, even in the case of a simple power-law source function, $\Delta N(\gamma) \propto E^{-\alpha}$, this approach does not lead to any convenient analytical result. Below we shall demonstrate that the direct solution of Eq. (1) for an arbitrary injection spectrum $\Delta N(\gamma)$ is possible as well without resorting to the Green's function technique with respect to the variable γ. Moreover this approach allows us to obtain a simple analytical formula convenient both for further qualitative analysis and quantitative applications.

Let us assume that at $t_0 = 0$ the CR's with an arbitrary energy spectrum $\Delta N(\gamma)$ are distributed uniformly in the source with a radius r_s. The propagation of these electrons in space at $t > 0$ is described by the homogeneous ($Q = 0$) diffusion Eq. (1) with initial distribution function

$$f_0(r,\gamma) = \frac{\Delta N(\gamma)}{(4\pi/3)r_s^3}H(r_s - r). \tag{2}$$

Here $H(x)$ is the Heaviside step function ($H = 0$ at $x < 0$, and $H = 1$ at $x > 0$). To solve Eq. (1), we define a new function $F = rPf$ and use a new variable T instead of γ:

$$T = \int_{\gamma}^{\gamma_\star} \frac{dx}{P(x)} = g(\gamma). \tag{3}$$

This variable is the time required for a particle to cool down from some fixed energy $\gamma_\star$ to energy γ. Note that formally the choice of the value of $\gamma_\star$ is arbitrary, and in the case of an energy-loss rate increasing faster than $P \propto \gamma$ the value of $\gamma_\star$ can be chosen infinitely large. In the case of a weaker energy-loss rate, $\gamma_\star$ may be taken as any large value, for example, as the maximum energy of particles injected into the ISM. In the variable T, Eq. (1) reads as

$$\frac{\partial F}{\partial t} = D_1(T)\frac{\partial^2 F}{\partial r^2} - \frac{\partial F}{\partial T}. \tag{4}$$

Here $D_1(T) = D(\epsilon)$, where $\epsilon \equiv \epsilon(T)$ is the inverse function to $g(\gamma)$ defined by Eq. (3), i.e., $\gamma = g^{-1}(T) \equiv \epsilon(T)$. Passing from the variables (t, T) to $(\tau = T - t, z = T)$, Eq. (4) is reduced to a partial differential equation in only two variables:

$$\frac{\partial \tilde{F}}{\partial z} = D_1(z)\frac{\partial^2 \tilde{F}}{\partial r^2}, \tag{5}$$

where $\tilde{F}(r,\tau,z) = F(r,t,T)$. The initial distribution function (2) at $t \to 0$ corresponds to the condition $\tilde{F}(r,z,\tau) \to \tilde{F}_0(r,\tau)$ at $z \to \tau$, with

$$\tilde{F}_0(r,\tau) = r\frac{H(r_s - r)}{(4\pi/3)r_s^3}\Delta N(\gamma)P(\gamma)|_{\gamma=\epsilon(\tau)}. \tag{6}$$

Finally, defining a new variable u,

$$u = \int_0^z D_1(x)dx, \tag{7}$$

instead of z, Eq. (5) is brought to the standard form of the homogeneous equation of diffusion with constant coefficients and initial function $\tilde{F}_0$ at $u \to u_0 = \int_0^\tau D_1(x)dx$. The solution to this equation on the semi-infinite line $r \geq 0$ is known (see [15]):

$$\tilde{F} = \frac{1}{2\sqrt{\pi \Delta u}}\int_0^\infty \left[\exp\left(-\frac{(r-x)^2}{4D\Delta u}\right) - \exp\left(-\frac{(r+x)^2}{4D\Delta u}\right)\right]F_0(x,\tau)dx, \tag{8}$$

where $\Delta u = u - u_0$. Letting $r_s \to 0$ we obtain the solution of Eq. (1) for the δ-function-type initial distribution of particles both in space and time, i.e., the Green's function with respect to r and t, for an arbitrary injection spectrum $\Delta N(\gamma)$:

$$f(r,t,\gamma) = \frac{\Delta N(\gamma_t) P(\gamma_t)}{\pi^{3/2} P(\gamma) r_{\rm dif}^3} \exp\left(-\frac{r^2}{r_{\rm dif}^2}\right). \tag{9}$$

Here $\gamma_t \equiv \epsilon(T-t)$ corresponds to the initial energy of particles which are cooled down to given γ during the time t, and

$$r_{\rm dif}(\gamma, t) = 2\sqrt{\Delta u} \tag{10}$$

corresponds to the effective diffusion radius up to which electrons with energy γ propagate during the time t after their injection from the source. When obtaining Eq. (9) we have used the equation $D_1(T)dT = D(\gamma)d\gamma/P(\gamma)$, which follows from Eq. (3) and the definition of $D_1(T)$. The dependence on t enters in Δu through γ_t:

$$\Delta u(\gamma, \gamma_t) = \int_\gamma^{\gamma_t} \frac{D(x)dx}{P(x)}. \tag{11}$$

Notice that at $t \to T$ the energy $\gamma_t \to \gamma_*(\to \infty)$ and for the particles with $T(\gamma) \le t$ the distribution function equals zero.

Equation (9) was obtained without any specification of the initial spectrum $\Delta N(\gamma)$, the energy losses $P(\gamma)$, or the diffusion coefficient $D(\gamma)$. Since the dependence of f on r in the Eq. (9) has a simple exponential form, this solution is convenient for integration for spatially distributed sources. Moreover, this distribution function can be easily integrated over a finite particle injection time as well, transforming the integration from dt to $d\gamma_t = P(\gamma_t)dt$ [this equation follows from the definition of $\gamma_t \equiv \epsilon(T-t)$ and Eq. (3), which result in familiar $t = \int_\gamma^{\gamma_t} dx/P(x)$]. For example, in the case of continuous injection of CR's from a stationary point source we can substitute $\Delta N(\gamma) \to Q(\gamma)dt$, and after integration of Eq. (9) over dt the resulting stationary distribution function reads

$$f(r,\gamma) = \frac{1}{8\pi^{3/2} P(\gamma)} \int_\gamma^\infty \frac{Q(x)}{[\Delta u(\gamma, x)]^{3/2}} \times \exp\left(-\frac{r^2}{4\Delta u(\gamma, x)}\right) dx. \tag{12}$$

In the case of stationary sources distributed uniformly in space at distances beyond some r_0 from us, we can substitute $Q(\gamma) \to q(\gamma)d^3r$ (q being the specific injection rate per unit volume) and integrate over the region $r > r_0$, which results in

$$f(\gamma) = \frac{1}{P(\gamma)} \int_\gamma^\infty q(x) \left[\operatorname{erfc}(a_0) + \frac{2a_0}{\sqrt{\pi}} e^{-a_0^2}\right] dx, \tag{13}$$

where $\operatorname{erfc}(z) = (2/\sqrt{\pi}) \int_z^\infty \exp(-x^2)dx$ is the error function (see [16]), and $a_0 = r_0/2\sqrt{\Delta u(\gamma, x)}$. Notice that, since $\operatorname{erfc}(0) = 1$, in the limiting case $r_0 \to 0$ this latter equation gives the familiar result for the distribution of particles which are injected stationarily and uniformly into interstellar space, and suffer continuous energy losses. In this case the dependence on D disappears at all.

III. THE ENERGY SPECTRUM OF RELATIVISTIC ELECTRONS

Consider now the energy-loss rate of relativistic electrons:

$$P(\gamma) = p_0 + p_1\gamma + p_2\gamma^2. \tag{14}$$

Here $p_0 = 2\pi(e^2/m_ec^2)^2 cA_i n \simeq 6 \times 10^{-13} n\ \mathrm{s}^{-1}$ is for the ionization losses ($A_i \sim 30$–50 being a weak logarithmic function of γ, e.g., [1]) of the electrons in a neutral interstellar gas with number density n (in units of cm^{-3}). The second term with $p_1 \simeq 10^{-15} n\ \mathrm{s}^{-1}$ corresponds to the bremsstrahlung energy losses (for relevant analytical expressions see [17]), and the last one, with

$$p_2 = 5.2 \times 10^{-20} \frac{w_0}{1\ \mathrm{eV/cm^3}}\ \mathrm{s}^{-1} \tag{15}$$

and $w_0 = w_B + w_{\rm MBR} + w_{\rm opt}$, represents synchrotron and inverse Compton losses ($w_{\rm MBR} = 0.25\ \mathrm{eV/cm^3}$ is the microwave background radiation energy density, $w_{\rm opt} \simeq 0.5\ \mathrm{eV/cm^3}$ stands for the energy density of optical-IR radiation in interstellar space; the energy density of the magnetic field $w_B = 0.6\ \mathrm{eV/cm^3}$ for $B = 5\mu$G). Notice that a more accurate expression for $P(\gamma)$ should take into account that the Compton scattering of electrons with energies $\gamma \ge 10^5$ off the optical photons corresponds to the Klein-Nishina limit rather than to the Thomson limit implied in Eq. (14). In our calculations, however, we neglect this effect (which does not significantly change the results below), and assume $w_0 \simeq 1\ \mathrm{eV/cm^3}$.

To find an analytical expression for γ_t entering the basic equations (9)–(11), we note that for $n/w_0 > 0.13\ (\mathrm{eV})^{-1}$ the equation $P(\gamma) = 0$ has two roots, at $\gamma = -\gamma_1$ and $\gamma = -\gamma_2$, respectively, where $\gamma_1 \simeq p_0/p_1 \simeq 600$ is the energy where the bremsstrahlung energy loss equals the ionization loss, and $\gamma_2 \simeq p_1/p_2 \simeq 1.9 \times 10^4 n(w_0/1\ \mathrm{eV\,cm^{-3}})^{-1}$ corresponds to the energy above which the Compton and synchrotron energy losses dominate bremsstrahlung. Then Eq. (14) is reduced to $P(\gamma) = p_2(\gamma + \gamma_1)(\gamma + \gamma_2)$, and Eq. (3) results in the following expressions for T and $\gamma_t = \epsilon(T-t)$:

$$T = \frac{1}{\nu} \ln \frac{\gamma + \gamma_2}{\gamma + \gamma_1}, \tag{16}$$

$$\gamma_t = \frac{\gamma + \gamma_1}{1 - (1 - e^{-\nu t})(\gamma + \gamma_2)/(\gamma_2 - \gamma_1)} - \gamma_1 \tag{17}$$

with $\nu \equiv p_2(\gamma_2 - \gamma_1) \approx p_1$. Note that the maximal time $T(\gamma)$ for cooling of electrons from infinity down to any energy γ cannot significantly exceed the bremsstrahlung loss time scale $t_{\rm br} = 1/p_1 \simeq 3 \times 10^7 n^{-1}$ yr. Equations (16) and (17) together with Eqs. (9)–(11) represent the solution of the diffusion equation of electrons with energy losses in the general form of Eq. (14).

For time scales $t \le 10^7$ yr (corresponding to the limit of $\nu t \ll 1$) only Compton and synchrotron energy losses of high-energy electrons, $\gamma \gg \gamma_2$, are important. In this case $\gamma_t \approx \gamma/(1 - p_2 t\gamma)$, and Eq. (9) reduces to

$$f(r,t,\gamma) = \frac{N_0\gamma^{-\alpha}}{\pi^{3/2}r^3}(1-p_2t\gamma)^{\alpha-2}\left(\frac{r}{r_{\rm dif}}\right)^3 e^{-(r/r_{\rm dif})^2}, \tag{18}$$

where $\gamma < \gamma_{\rm cut} \equiv \gamma_{\rm cut}(t) = (p_2t)^{-1}$ (otherwise $f = 0$), and

$$r_{\rm dif}(\gamma,t) \simeq 2\sqrt{D(\gamma)t\frac{1-(1-\gamma/\gamma_{\rm cut})^{1-\delta}}{(1-\delta)\gamma/\gamma_{\rm cut}}}. \tag{19}$$

Here we assume the power-law distribution $\Delta N(\gamma) = \Delta N_0\gamma^{-\alpha}$. In addition to this we suppose a power-law dependence of the diffusion coefficient at high energies: $D(\gamma) \propto \gamma^\delta$. However, at energies below several GeV this is probably no more true, and it seems more reasonable (see the discussion section for physical arguments) to choose $D(\gamma)$ which becomes constant at low energies. To take this effect into account, we assume

$$D(\gamma) = D_0(1+\gamma/\gamma_*)^\delta \tag{20}$$

with $\gamma_* \leq 10^4$. This form allows a *gradual* change of the behavior of the diffusion coefficient at $\gamma \sim \gamma_*$ to a constant value D_0 for $\gamma \ll \gamma_*$.

From Eq. (19) follows that already at energies $\gamma \leq 0.5\gamma_{\rm cut}$ the diffusion radius comes to $r_{\rm dif} \simeq 2\sqrt{D(\gamma)t}$, and Eq. (18) reduces to the familiar expression for CR diffusion [with arbitrary $D(\gamma)$] without energy losses (e.g., see [1]). This means that, although Eqs. (18) and (19) have been initially obtained for electrons with $\gamma > \gamma_*$, they are valid at energies $\gamma \leq \gamma_*$ as well, until $t \leq 10^7$ yr (i.e., when only Compton and synchrotron energy losses may be taken into account).

It is worth noticing that in the case of energy-independent diffusion (i.e., $\delta = 0$) Eqs. (18) and (19) come to the solution obtained earlier by Berkey and Shen [18], which has been used further on by Shen [7] and Shen and Mao [8] to analyze the spectra of high-energy CR electrons from nearby sources. A similar analysis has been done also by Cowsik and Lee [9]. We should emphasize, however, that in those earlier studies only the energy-*independent* diffusion was considered. In this particular case the spectra of electrons injected into the ISM from a point source, and reaching the observer at different times, just repeat (except for the abrupt cutoff at $\gamma \geq \gamma_{\rm cut}$) in their form the primary spectra of electrons. As it follows from our analysis below, energy-*dependent* diffusive propagation results in a significant *modification* of the nonstationary energy spectra of electrons. Notice that this very feature becomes the key point for the subsequent explanation of both the energy spectra and the charge composition of CR electrons observed.

It follows from Eqs. (18) and (19) that starting only from energies $\gamma > 0.5\gamma_{\rm cut}$ the energy losses become significant, resulting in sharp cutoff of the spectra of electrons at $\gamma \geq \gamma_{\rm cut}$. Since this transition takes place in a rather narrow energy range, $\gamma = (0.5\text{–}1)\gamma_{\rm cut}$ (see Fig. 1), one can for purposes of practical analytical calculations use very convenient formulas for $f(r,t,\gamma)$ and $r_{\rm dif}$ without energy losses up to $\gamma \leq a\gamma_{\rm cut}(t)$ with, say, $a \approx 0.75$, and assume an abrupt cutoff of the spectrum above that energy. This approximation is used to derive Eq. (21) below.

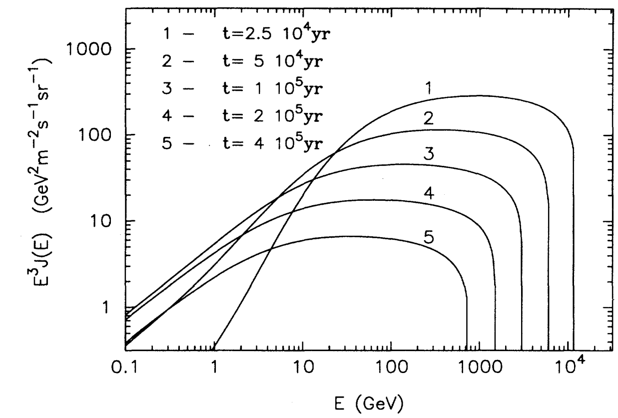

FIG. 1. The energy spectra of electrons at different times t after their injection into the ISM from a source at distance $r = 100$ pc. The calculated spectra correspond to a total energy output $E_{\rm tot} = 10^{48}$ erg in power-law primary electrons, $\alpha = 2.2$, extending up to $\gamma_{\rm max} = 10^9$; parameters of the diffusion coefficient are $\delta = 0.6$, $D_{10} \equiv D(10 \text{ GeV}) = 10^{28}$ cm^2/s, and $E_* = m_ec^2\gamma_* = 3$ GeV; a total energy output $E_{\rm tot} = 10^{48}$ erg is assumed.

From Eq. (18) follows that at given energies $\gamma(< \gamma_{\rm cut})$, an observer at a distance r from the source would observe the maximal flux of electrons, $J = cf/4\pi$, at times $t_{\rm max}(\gamma) = r^2/6D(\gamma)$ after their injection, when $r_{\rm dif}(\gamma,t) = \sqrt{2/3}\,r$. At $t \ll t_{\rm max}$ the electrons of these energies have not yet reached the observer, while at $t \gg t_{\rm max}$ the maximum flux of the electrons has already passed by, and their density decreases due to spherical diffusive expansion as $r_{\rm dif}^{-3} \propto t^{-3/2}$. It is worth noting also that, while the magnitude of the maximal flux at $t \sim t_{\rm max}$ essentially depends on the distance r, it becomes independent of r at times $t \gg t_{\rm max}$. In the case of energy-independent diffusion a similar qualitative analysis of the time dependence of the spectra of CR's from a single source has been done earlier by Lingenfelter [12]. The essential difference is that for the energy-dependent diffusion the time $t_{\rm max}$ of the maximal flux of electrons is different for electrons with different energies, which results in a significant time-dependent modification of the spectra of primary particles.

Except for the abrupt cutoff at energies $\gamma > \gamma_{\rm cut}(t)$, the modification of the energy spectra of electrons as compared with the primary spectra, is described by the factor $G(\gamma,t) = s^3e^{-s^2}$, and depends only on one parameter, $s = r/r_{\rm dif}$. For energy-independent diffusion ($\delta = 0$) this parameter is energy independent as well. Therefore in this case the primary spectra of electrons are not modified by diffusion, and the only consequence of propagation of electrons (or CR's) from a point source is reduced to the time-dependent suppression factor G alone.

Considering now the general case of energy-dependent diffusion, we emphasize that the energy spectra of electrons at any instant t and distance r are essentially modified due to the propagation of electrons with different rates at different energies. In particular, assuming first the case of burstlike injection (i.e., when the duration of injection of electrons into the ISM is significantly shorter than the observation time t), note that in the high-energy range satisfying the condition $r/r_{\rm dif} \leq 0.5$, i.e., for

$$\gamma \geq \gamma_c = \max\left(\gamma_*, \gamma_* \times [(r^2/D_0 t)^{1/\delta} - 1]\right)$$

and up to $\gamma \leq \gamma_{\rm cut}(t)$, the electrons are distributed by a power law with the exponent $\alpha' = \alpha + \frac{3}{2}\delta$. At energies $\gamma \ll \gamma_c$ and down to $\gamma \sim \gamma_*$ the primary spectrum is exponentially modified (*suppressed*), and at $\gamma \ll \gamma_*$ where $D(\gamma) \approx$ const, the electrons reaching the observer repeat the power-law shape of the primary (injection) energy spectrum although with essentially suppressed amplitude. All the spectral features discussed above can be recognized in Fig. 1 where the temporal behavior of the electron flux at distance $r = 100$ pc from the source is shown.

In the case of continuous injection of electrons from a point source the energy spectrum of electrons is qualitatively different. For example, assuming injection with a constant rate during the time $0 \leq t' \leq t$, in Eq. (18) we can substitute $N_0 \to Q_0 dt'$ and integrate over dt' arriving at the energy spectrum

$$f_{\rm st}(r,t,\gamma) = \frac{Q_0 \gamma^{-\alpha}}{4\pi D(\gamma) r} \text{erfc}\left(\frac{r}{2\sqrt{D(\gamma) t_\gamma}}\right), \qquad (21)$$

where

$$t_\gamma = \min\left(t, a/(p_2 \gamma)\right). \qquad (22)$$

At low energies the behavior of Eq. (21) is similar to Eq. (18) for burstlike injection. However, at higher energies it is qualitatively different. In particular, the steepening of this spectrum at high energies corresponds to a power-law index $\alpha' \approx \alpha + \delta$. In addition to this, the cutoff of the energy spectrum above $\gamma_{\rm cut}$ expected in the case of burstlike injection, now disappears.

IV. VALIDITY OF THE CONTINUOUS SOURCE DISTRIBUTION APPROACH

The standard interpretation of the fluxes of CR electrons is based on the assumption of a continuous and uniform distribution of the sources in the Galaxy. Both *leaky-box* and *diffusion* models satisfactorily explain the observed energy spectrum of electrons (e.g., [11,19]). An example of a typical fit to the experimental data in the framework of these models is presented in Figs. 2(a) and 2(b) (solid curves). In the case of stationary injection of electrons into the ISM from the sources continuously distributed in the Galaxy, the equilibrium spectrum of electrons depends weakly on the real geometry of the source distribution, the main modification of the primary spectrum being due to energy losses. In particular, in the energy region $0.3 < E < 10$ GeV where bremsstrahlung energy losses dominate, the distribution of electrons in the ISM can be described as a power law with the exponent of the primary electrons, $\alpha' \approx \alpha$. In the high-energy region $E > 10$ GeV, where the Compton and synchrotron losses ($P \propto \gamma^2$) dominate, the spectrum steepens to $\alpha' = \alpha + 1 - \Delta$, where Δ is a small correction term depending on the real geometry of the spatial distribution of the sources. For example, in the case of a homogeneous spherical distribution of the sources the term $\Delta = 0$, which readily follows from Eq. (13) for $r_0 = 0$. In the case of a homogeneous two-dimensional distribution (i.e., in the Galactic plane) of stationary sources,

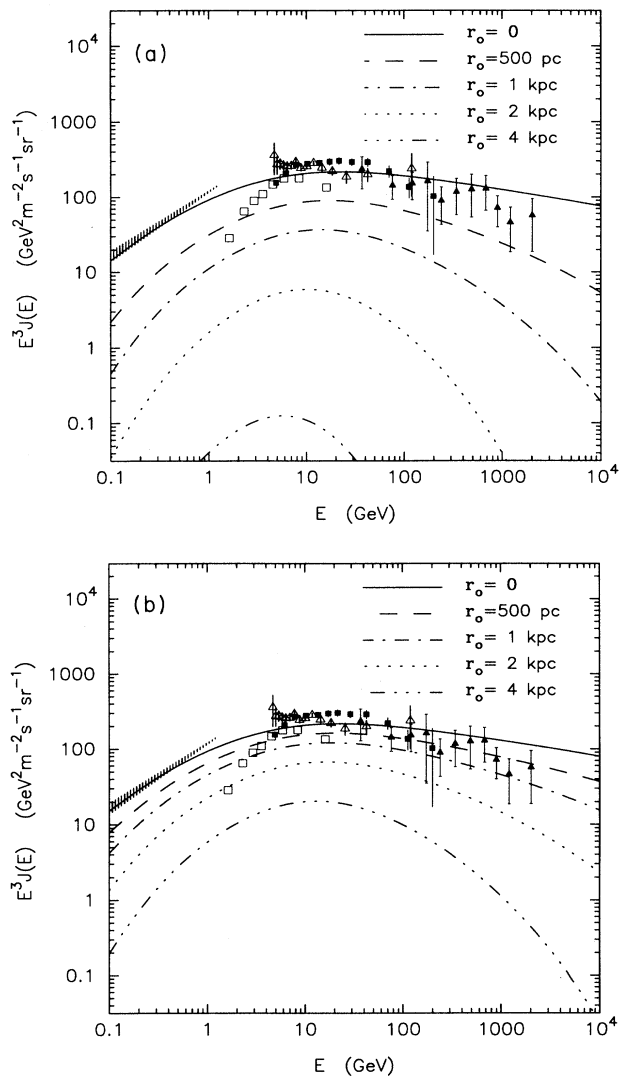

FIG. 2. The fluxes of electrons from sources continuously and uniformly distributed in the galactic disk, calculated for parameters $\alpha = 2.4$, $\delta = 0.6$, $E_* = 3$ GeV, and two different absolute values of the diffusion coefficient corresponding to (a) $D_{10} = 10^{28}$ cm^2/s, and (b) $D_{10} = 10^{29}$ cm^2/s. The total spectra (solid lines) are decomposed to show the spectral fluxes (contributions) coming from the sources at distances $r \geq r_0$. The experimental fluxes correspond to the measurements by Taira *et al.* [11] (shown by solid triangles), Tang [19] (solid squares), Golden *et al.* [20] (open triangles), and Basini *et al.* [21] (open squares). The dashed region corresponds to the fluxes of CR electrons deduced from radio observations by Webber *et al.* [22].

integration of Eq. (12) results in

$$f(\gamma) \propto \frac{1}{P(\gamma)} \int_{\gamma}^{\infty} \frac{q(x)}{\sqrt{\Delta u(\gamma, x)}} dx. \tag{23}$$

Since at high energies the diffusion coefficient $D(\gamma) \propto \gamma^{\delta}$, we have $\Delta u(\gamma, x) \propto (\gamma^{\delta-1} - x^{\delta-1})$. Therefore, integration of Eq. (23) results in the factor $\Delta = (1-\delta)/2$. Thus, in order to fit the measured power-law energy spectrum of CR electrons with index $\alpha' \approx 3.1$–3.3, an injection spectrum with $\alpha = 2.4$ and two different diffusion coefficients with the same exponent $\delta = 0.6$ are assumed for the spectra presented in Figs. 2(a) and 2(b). The solid curves in these figures are calculated by integration of Eq. (12) assuming uniform distribution of the sources in the Galactic disk with thickness 300 pc. It is seen that indeed there is only a weak different in the shapes of these two curves. However, for different diffusion rates the partial contributions to the total electron flux from sources at different distances are different. This is demonstrated in Figs. 2(a) and 2(b), where the total energy spectra (solid curves) are decomposed to show the contributions from sources located at distances $r \geq r_0$ for successively larger values of r_0.

It follows from Figs. 2(a) and 2(b) that the major fraction of the total electron flux comes from relatively close sources, $r \leq 0.5$–1 kpc. This means that the hypothesis of a continuous distribution (both in space and time) of sources should be valid first of all within the nearest several hundreds of parsecs. But can this be justified *a priori*? This hypothesis is certainly correct for electrons of the secondary origin, i.e., for those produced by CR protons and nuclei interacting with the ambient gas at each point of the interstellar medium. However, these secondary electrons (after $\pi^{\pm}$ decays) are not able to explain quantitatively the observed fluxes. Therefore directly accelerated electrons (e^-) are needed, and in order to satisfy the requirement of continuity, the mean distance between the sources of primary electrons should be $\ll 1$ kpc. Otherwise, the correct approach to the problem should consist of a two-component treatment of the observed fluxes to separate the distant and the nearby sources.

(1) The contribution from the galactic sources at large distances (hereafter, G component), typically $r \geq 1$ kpc, can still be treated in the framework of the assumption of a continuous source distribution both in space and in time. Assuming a spherically symmetric diffusion region for CR's, the energy spectra of electrons from these sources can be calculated, integrating Eq. (12) over a given geometry of sources starting from $r_0 \geq 1$ kpc.

(2) The contribution from one or several nearby and relatively young sources in the local environment should be treated separately (hereafter, L component). In this case both nonstationary and stationary scenarios for injection of accelerated particles into the ISM are possible; relevant calculations can be done using Eq. (9) or Eq. (12), respectively.

Note that this approach becomes particularly important for the interpretation of fluxes of high-energy electrons which suffer intensive radiative losses. Indeed, detection of CR electrons beyond 1 TeV implies the existence of at least one relatively young ($t \leq t_{\rm cool} \sim 10^5$ yr) source nearby. For typical values of the diffusion coefficient $D \sim (1$–$10)\times 10^{28}$ cm^2/s the characteristic distance to the source is estimated as $r \leq r_{\rm dif} \approx 2\sqrt{Dt} \sim 100$–$300$ pc. In the next section we show that the superposition of energetic (e^+, e^-) pairs injected into the ISM from a source at distance $r \sim 100$ pc at times $t \leq 10^5$ yr, and of negatrons (e^-) produced in distant galactic sources, can naturally account for both the very specific energy dependence of the positron content [i.e., of the ratio $e^+/(e^- + e^+)$], and of the observed electron flux.

V. ENERGY SPECTRA AND POSITRON CONTENT IN THE TWO-COMPONENT APPROACH

In Fig. 3(a), the energy spectrum of electrons from distant sources distributed uniformly and continuously beyond 1 kpc in the galactic disk (the G component, full dots), and the spectra of electrons from a single local source (L component) at distance $r = 100$ pc for three different times of injection are presented. The spectra of the L component correspond to "burstlike" injection, i.e., when the duration of the effective production of electrons injected into the ISM is much less than the age of the source, $t \sim 10^5$ yr. For the case of $t = 10^5$ yr the total $(G + L)$ spectrum is also plotted (thick solid line). Though the diffusion coefficient may be different in different parts of the ISM, we suggest the same diffusion coefficient for both the G and L components. The curves are calculated assuming the diffusion coefficient with $\delta = 0.6$ and $E_* = 2$ GeV in Eq. (20), and choosing D_0 so that $D_{10} \equiv D(10 \text{ GeV}) \sim 10^{28}$ cm^2/s. These suggestions have a certain theoretical background (see, e.g., [1,2]), and are consistent with the CR spectrum and chemical composition measurements [23]. Our numerical study shows that for a good fit to both electron and positron data, the value of the parameter $s = r/r_{\rm dif}$ should be in a rather narrow range (within a factor of ≤ 2) around 1 at $E = 10$ GeV. The spectra in Fig. 3(a) are calculated assuming $D_{10} = 0.7 \times 10^{28}$ cm^2/s, such that $s(10 \text{ GeV}) = 1$ for $t = 10^5$ yr. The spectra are normalized to the observed total flux of electrons at $E = 10$ GeV.

Another important parameter which characterizes high-energy electrons is the ratio $C_+ \equiv e^+/(e^- + e^+)$. The reported experimental results shown in Fig. 3(b) indicate a general behavior in the form of an increase of C_+ with energy above several GeV. This behavior as well as the absolute values of the positron fluxes cannot be attributed to the production of secondary positrons due to interactions of cosmic-ray protons and nuclei with interstellar gas [3]. In the framework of the proposed two-component model this effect can be easily explained assuming a pure negatron composition for the G component, and an equal amount of negatrons and positrons for the L component. The results of the calculations are shown in Fig. 3(b). We have normalized the sum of the theoretical G and L spectra to the measured flux, and the theoretical positron-to-electron ratio, $0.5L/(G + L)$, to the measured one at energy $E = 10$ GeV. At high energies, $E \geq 10$ GeV, the increase of the positron content C_+ is connected both with the increase (in the $J \times E^3$ plot) of the positron flux from the nearby source, and the decrease of the spectrum of negatrons from distant sources due to strong Compton and synchrotron losses. In the energy range $E \leq 1$ GeV the increasing positron content is connected with the fast drop of the flux of e^- from distant sources. Indeed, the diffusion time of low-energy electrons, $E \ll 10$ GeV, from distances $r > 1$ kpc is comparable with the characteristic energy loss times due to bremsstrahlung and ionization processes, so that the G-component flux of the low-energy electrons also is significantly suppressed.

This very effect allows us to fit the measured spectrum of electrons below a few GeV, while the standard models which assume a continuous spatial distribution of the sources at all length scales (formally even infinitely close to us) result in fluxes of low-energy electrons which conform with the ones derived from the radio data, and are significantly higher than the locally measured ones (see, e.g., [22]). In the framework of the proposed model this discrepancy is readily understood. Indeed, our model does not exclude high electron densities in different locations of the Galaxy, which follows from the radio data (providing information on the low-energy electron densities *averaged* along the line of sight). The key point is that these low-energy electrons, $E \ll 10$ GeV, similar to the electrons of very high energies, $E \geq 100$ GeV, reach us from large distances suffering significant energy losses. In fact, only the electrons in a relatively narrow energy range $E \sim$ (10–100) GeV are effectively reaching us from distances beyond 1 kpc.

In the case of burstlike injection a prominent feature of the energy spectra of electrons is a sharp cutoff at energies $E \geq E_{\text{cut}} = m_e c^2 \gamma_{\text{cut}}$ depending on the age of the local nearby source [see Fig. 3(a)]. As we discussed in Sec. III, this feature is absent if the source would efficiently produce high-energy electrons during a time interval comparable with its age. This can be seen in Fig. 4 where the dashed line corresponds to the energy spectra of electrons from the source of age $t = 10^5$ yr located at distance $r = 100$ pc stationarily injecting into the ISM relativistic (e^+, e^-) pairs with a power-law exponent $\alpha = 2.2$. An exponent $\delta = 0.6$ in the diffusion coefficient in Eq. (20) is assumed. The spectrum is normalized to the measured flux of positrons at $E = 10$ GeV, which

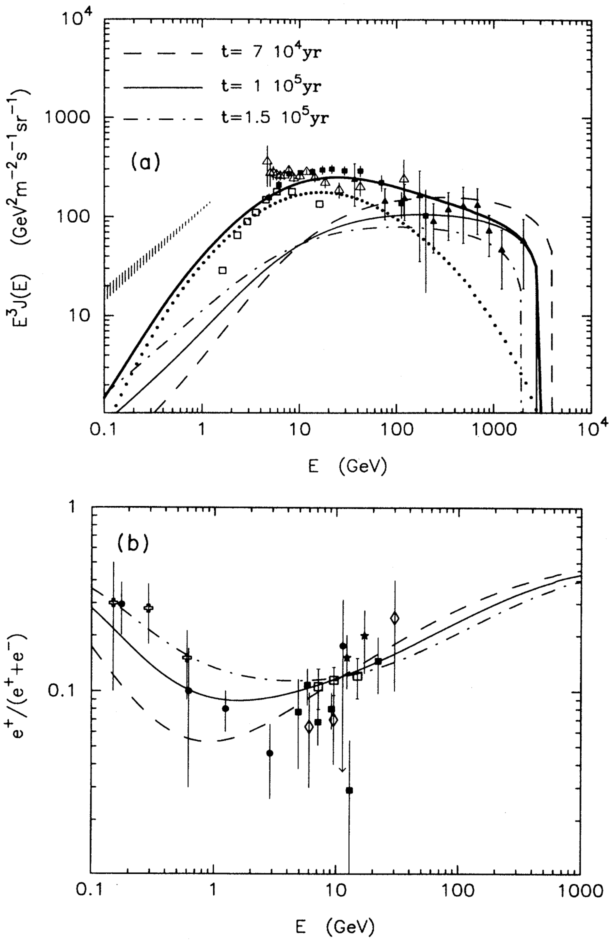

FIG. 3. (a) The energy spectra of the G component (solid dots) and of the L component assuming burstlike injection of electrons from the source of age t at the distance $r = 100$ pc. The L-component spectra calculated for three different values of t around 10^5 yr are presented. For one of these ages, $t = 10^5$ yr, the total spectrum of electrons is also presented (heavy solid line). The curves presented correspond to model parameters $\alpha = 2.2$, $\delta = 0.6$, $E_* = 2$ GeV, $D_{10} = 7 \times 10^{27}$ cm^2/s. The spectra are normalized to the observed flux of electrons and positrons at $E = 10$ GeV. (b) The charge composition of CR electrons/positrons for the spectra presented in (a). A pure negatron composition for the G component, and an equal amount of positrons and negatrons in the L component are assumed. The experimental data are from [21] (open squares), [24] (solid circles), [25] (crosses), [26] (diamond), [27] (stars), and [28] (solid squares).

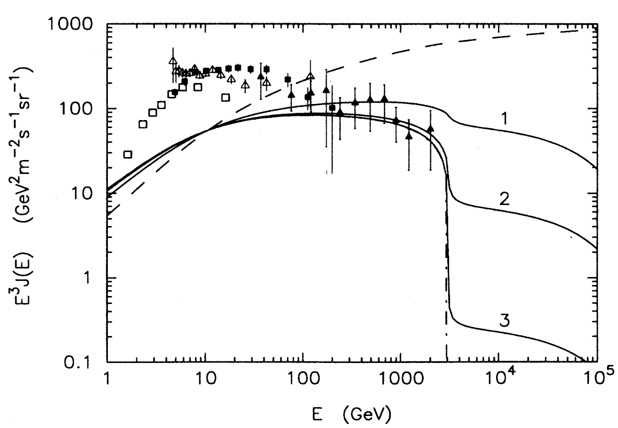

FIG. 4. The energy spectra of the L component normalized to the observed flux of positrons at $E = 10$ GeV for different types of injection: stationary (dashed line), burstlike (dot-dashed line), and continuous with injection rate proportional to magnetic dipole spin-down luminosity of pulsar (solid lines, see text for details). An age $t = 10^5$ yr and a distance $r = 100$ pc is assumed.

requires the luminosity of this source in primary (e^+, e^-) pairs to be $L_e = 2 \times 10^{36}$ erg/s. This corresponds to the injection of $E_{\rm tot} = 6.4 \times 10^{48}$ erg during $t = 10^5$ yr. It is worth noticing that in the case of burstlike injection (dot-dashed line in Fig. 4) the total energy output in primary electrons providing the same flux of positrons at 10 GeV is almost the same, $E_{\rm tot} = 6.2 \times 10^{48}$ erg. It is obvious from Fig. 4 that the flux of electrons from the stationary source of positrons would exceed the observed flux already at energies ≥ 100 GeV (provided we would not assume a steepening of the primary spectrum at high energies).

In the general case of continuous injection, intermediate between burstlike and stationary types, the high-energy spectra of the L component may combine the characteristic features of both these types. The solid lines in Fig. 4 represent the fluxes of electrons from the source at the same distance $r = 100$ pc and of age $t = 10^5$ yr continuously injecting relativistic electrons with the power-law index $\alpha = 2.2$ into ISM, but with the total luminosity varying in time during $0 \leq \tau \leq t$ as

$$L_e(\tau) = \frac{L_0}{(1+\tau/\tau_*)^k} \tag{24}$$

for three different values of the characteristic "decay" time τ_*: $\tau_*/t = 0.1$ (curve 1), $\tau_*/t = 0.01$ (curve 2), $\tau_*/t = 0.001$ (curve 3). This kind of time-dependent injection would correspond, in particular, to (e^+, e^-) pair production by a pulsar assuming that a definite fraction of its spin-down luminosity $L_{\rm SD}(\tau)$ is converted into relativistic electrons (note that the efficiency $\eta = L_e/L_{\rm SD}$ of electron acceleration may be very high; for example, for the Crab pulsar the efficiency $\eta \to 1$ is discussed [29]). The spectra presented in Fig. 4 are calculated for the exponent $k = 2$ in Eq. (24), corresponding to the temporal behavior of $L_{\rm SD}$ in the framework of the magnetic dipole (oblique rotator) model for pulsars [30,31]. In this case integration of $L_e(\tau)$ over time results in the total energy output $E_{\rm tot} = L_0\tau_*$, and exactly half of this energy is emitted during the high state of the source $\tau \leq \tau_*$.

As it is seen from Fig. 4, the characteristic feature of the energy spectra of electrons resulting from this time-dependent injection is the abrupt drop at energies $E \approx E_{\rm cut}(t)$ depending on the age of the source. The amplitude of the drop essentially depends on the duration of the characteristic time τ_* of effective production of relativistic electrons. In the case of large $\tau_*/t \sim 0.1$ this depth is relatively small (curve 1), since in this case still a significant fraction of electrons of very high energies is just freshly produced, at times $\leq 10^4$ yr. For shorter τ_* the cutoff is more pronounced. The initial luminosities L_0 in Eq. (24), normalized to the observed flux of positrons at 10 GeV, are equal to 2.0×10^{37} erg/s, 1.94×10^{38} erg/s, and 1.9×10^{39} erg/s for the curves 1, 2, 3, respectively, resulting in the same total energy output $E_{\rm tot} \approx 6 \times 10^{48}$ erg as in the cases of burstlike or stationary injections.

We point out that in the framework of the magnetic dipole model of the pulsar the "decay" time $\tau_* = t(\Omega/\Omega_i)^2$, where Ω and Ω_i are the present and initial angular velocities of the pulsar, respectively (e.g., see [32]). On the other hand, the decline of the energy spectrum of the electrons after the drop significantly depends on the magnitude of the exponent k in Eq. (24). It means that measurements of the very high energy spectra of electrons might provide very important information on the history of the local source of TeV electrons.

VI. DISCUSSION

The conventional interpretation of the energy spectrum of cosmic-ray electrons assumes a uniform and continuous distribution of sources in the Galaxy, both in space and time. Whereas for the protons and nuclei this assumption may be considered as a reasonable working hypothesis, the validity of this approach is strongly limited for high-energy electrons. The lifetime of relativistic electrons in the interstellar medium against synchrotron and inverse Compton losses is

$$t_c = E/(-dE/dt) \approx 3 \times 10^8 (E/1\ {\rm GeV})^{-1}\ {\rm yr}.$$

Thus the age of the observed TeV electrons cannot significantly exceed 10^5 yr which implies, for conventional values of the diffusion coefficient, the existence of a nearby source(s) at a distance $r \leq 2\sqrt{Dt} \sim$ 100–300 pc. This means that the hypothesis of a continuous distribution (both in space and time) of sources needs to be valid within the nearest several hundreds of parsecs. This hypothesis is formally correct for electrons of secondary origin, i.e., for those produced by CR protons and nuclei interacting with the ambient gas at each point of the interstellar medium. However, since the observed ratio $e^+/(e^- + e^+)$ is less than 0.5, the secondary electrons alone cannot be responsible for the observed fluxes. Therefore, directly accelerated electrons (e^-) are needed, and in order to satisfy the requirement of continuity, the mean distance between the sources of primary electrons should be ≤ 100 pc. Otherwise, the correct approach to the problem should separate the contributions from the distant and the nearby accelerators of electrons.

The cornerstone for the proper interpretation of the observed differential spectrum of electrons, especially of its high-energy part, is the *modification* of the nonstationary spectra of primary electrons due to energy-dependent diffusive propagation from a single source. Indeed, as it follows from Eqs. (18) and (19), or more generally from Eqs. (9) and (10), the modification of the spectra of primary particles is defined mainly by one parameter $s = r/r_{\rm dif}$ which depends both on time t and energy $E = m_e c^2 \gamma$. At energies below the maximum energy possible for the electrons of given age, $E \ll E_{\rm cut} = m_e c^2/p_2 t$, the diffusion radius in Eq. (19) reduces to $r_{\rm dif} \simeq 2\sqrt{D(E)t}$, and $s \simeq r/2\sqrt{D(E)t}$.

In the case of burstlike injection, the primary power-law spectrum of electrons at high energies, satisfying condition $r_{\rm dif} \gg r$ (i.e., $s \ll 1$), is steepened by a factor $\frac{3}{2}\delta$ which results in a power-law distribution with exponent $\alpha' = \alpha + \frac{3}{2}\delta$. Note that this steepening is due to the spherical energy-dependent diffusive expansion where electrons with different energies occupy different volumes $\sim r^3_{\rm dif}(E,t) \propto E^{(3/2)\delta}$. For the exponent $\delta \sim$ (0.5–0.6) in

Eq. (20), it means that the energy spectra of the L component will be in compliance with the measured fluxes of the very high-energy electrons, $E \geq 100$ GeV, described by the exponent $\alpha_{\rm obs} \approx$ (3.1–3.3), assuming primary spectra with $\alpha \approx$ (2.2–2.3). Since at these energies the arrival (diffusion) time of electrons from distances $r \geq 1$ kpc exceeds the radiative cooling time, the contribution of the G component to the observed flux of electrons is essentially suppressed [see Fig. 3(a)].

With decreasing energy the magnitude of the parameter s gradually increases to $s \approx 1$ at $E = 10$ GeV, and to $s > 1$ at smaller energies down to $E \sim E_* \geq 1$ GeV. It means that we are observing the picture when the main fraction of electrons of energies $E \ll 10$ GeV from the nearby source has not yet reached us, while due to faster propagation the electrons with $E \gg 10$ GeV are presently spread over distances $r_{\rm dif}$ well beyond the distance to the source. This leads to the increasing contribution of the L component in the measured flux of electrons with increasing energy in the range $E \geq 10$ GeV. At the same time, since at these energies the electron cooling time $t_c \propto 1/E$ decreases more quickly than their diffusion time $t_{\rm dif} \propto E^{-\delta}$, the G-component flux from distant sources (consisting predominantly of negatrons) becomes less prominent. Thus, at energies $10 \leq E \leq 100$ GeV, a gradual replacement of the fluxes of the G component by those of the L component takes place. This transition from the G-component electrons to the L-component electrons occurs smoothly, therefore it is not seen in the total $G + L$ spectrum which can be well described in terms of a unique power-law distribution in the entire energy range 10 GeV $< E \leq 2$ TeV [see the heavy solid line in Fig. 3(a)]. However, if the charge composition of the L component is different from the one of the G-component electrons, then the transition from the G-component to the L-component electrons will be seen in the ratio $e^+/(e^- + e^+)$. In this case above 10 GeV one has to expect strong increase of the $e^+/(e^- + e^+)$, reaching the value 0.5 at energies $E \sim 1$ TeV [see Fig. 3(b)]. This would happen if the nearby source is a pulsar accelerating (e^+, e^-) pairs, while the bulk of electrons is directly accelerated by shocks of supernova remnants as generally believed.

At energies $E \sim 10$ GeV the ratio $t_c/t_{\rm dif}$ of cooling to diffusion times reaches its maximum. Therefore at these energies the electrons produced in distant galactic sources reach us most efficiently (obviously, at $t_{\rm dif} \geq t_c$ the electron fluxes are significantly suppressed due to energy losses). At smaller energies the ratio $t_c/t_{\rm dif}$ decreases again. In the energy region of several GeV, where the bremsstrahlung energy losses dominate (i.e., $t_c \sim t_{\rm br} \approx$ const), this is connected with the decrease of the diffusion coefficient, gradually flattening at $E \leq E_*$. At energies $E \leq 1$ GeV, where the diffusion becomes energy independent, the further decreases of $t_c/t_{\rm dif}$ is due to the increasing contribution of ionization losses, with $t_{\rm ion} \propto E$. All this results in energy spectra of the G component at $E \ll 10$ GeV which are significantly flatter (in the $J \times E^3$ plot, decreasing faster) than the primary spectra of electrons. Thus, the decrease of the ratio $t_c/t_{\rm dif}$ with decreasing energy at $E \ll 10$ GeV explains the discrepancy between the spectrum of electrons derived from the radio data (which provide the information on the CR electron density integrated along the line of sight) and the measured spectrum below a few GeV [see Fig. 3(a)]. Note that the leaky-box or diffusion models which assume continuous distribution of sources in the Galaxy, predict at low energies fluxes which are significantly higher than the observed fluxes [see Figs. 2(a) and 2(b)]. Since this disagreement extends up to a few GeV, it hardly could be attributed to the effect of modulation of electrons in the heliosphere.

It should be emphasized that the assumption of energy-dependent diffusive propagation is crucial for explanation of the experimental data by the suggested two-component model. Indeed, since the energy losses of electrons with $E < 1$ TeV during the propagation time $t \leq 10^5$ yr (which follows from the observation of $E > 1$ TeV electrons) from a single source are negligible, the energy-independent diffusion coefficient would require an injection spectrum of primary electrons $\propto E^{-3.1}$. This spectrum seems to be not only unrealistic for the injection spectrum, but, more importantly, would lead to contradiction with the observed flux below 10 GeV. The modification (steepening) of the primary spectrum of electrons from a single nearby source is possible only due to the diffusive *energy-dependent propagation* effect.

Our arguments for a diffusion coefficient in the form of Eq. (20) are as follows. Analyzing the secondary to primary ratio of CR nucleons in the so-called leaky-box approximation, equivalent to pure spatial diffusion in a fixed confinement region, results in a scattering mean free path $\lambda(p)$ that increases with decreasing energy below rigidities of order 1 GV [33], in contrast to our assumed flattening of $D(E)$. This model-dependent interpretation is however far from unique. Adding the physical process of diffuse interstellar reacceleration of primaries (and secondaries as well), originally produced in sources such as supernova remnants (SNR's), results not only in a weaker rigidity dependence of $\lambda(p)$ at higher energies, but allows even a monotonic decrease of $\lambda(p)$ with the momentum p for all p of interest here [34]. We should like to comment that at least two effects are still not taken into account in these arguments. First of all CR particles will not only diffuse but also convect if the Galaxy has a wind which is called for by dynamical arguments [35]. This affects low rigidity particles strongly because their diffusion is so slow. Thus, in a pure diffusion or a leaky-box picture a wind will show up in $D(E)$ becoming constant at low rigidities. This is the only way to simulate (rigidity independent) convection by diffusion. The second effect is that diffuse reacceleration depends on the existence of a wave spectrum that contains waves propagating parallel to the mean interstellar magnetic field as well as waves propagating in the antiparallel direction. This can only be true in the Galactic disk where stellar mass loss in the form of supernova explosions and stellar winds produces random ("turbulent") gas motions. In the much more extended Galactic halo beyond the disk these wave sources are "below" and lead to outgoing waves only, to lowest order. The same is true for waves self-generated by the CR gradient *in situ*. Thus, to lowest order, there is no reacceleration in the halo at all. In the disk, in addition, magnetohydrodynamic (MHD) waves are damped on the neutral gas. All this diminishes the effect of reacceleration in general. What is left of it is mainly effective for the low-energy nucleons observable at the solar system: they cannot come from the halo due to the convective removal but rather from the disk only, and for that matter, must come from fairly nearby.

With all these arguments in mind, it appears most reasonable physically to choose a $D(E)$ for electrons which becomes constant at low energies, and has a strong energy dependence $D(E) \propto E^{\delta}$. Our preferred parameters are $\delta \approx 0.6$ and thus $\alpha = 2.2$ to 2.3, corresponding to a hard source spectrum. We should point out, however, that even a smaller value of δ, say equal to 0.3 in Eq. (20), would make only a minor quantitative difference to our arguments, provided one can chose a soft ($\alpha \simeq 2.7$) electron source spectrum.

Discussing the most probable range of distances to the nearby source, and the energetics of this source required, we note the following. To fit the data, the magnitude of parameter s at 10 GeV should be within a rather narrow range around 1. As follows from Eq. (18), for fixed values of $r/r_{\rm dif}$ the absolute values of the fluxes at given energies would decrease $\propto r^{-3}$ with increasing distance r from the source. In the case of directly accelerated primary electrons with $\alpha \simeq 2.2$ the total energy output in relativistic electrons for the source at distance $r = 100$ pc is about $E_{\rm tot} \approx (0.5\text{–}1) \times 10^{49}$ erg. Suggesting the source at a distance only three times larger, $r = 300$ pc, we would have to suppose the energy output in relativistic electrons to be as high as $E_{\rm tot} \sim (1\text{–}2) \times 10^{50}$ erg, corresponding to the upper limit of reasonable values of the energy output in relativistic particles that could be produced by a single source (such as a supernova remnant or a pulsar). Therefore, the distance to the source can hardly exceed 300 pc. On the other hand, assuming the distance $r = 50$ pc, we could reduce the required energetics of the source below 10^{48} erg. Reducing the distance r, we have to reduce also the product $D_{10} \times t \approx r^2/4$. Thus, in the case of distances well below 50 pc, we have to suggest that either the nearby source is much younger than 10^5 yr or the diffusion coefficient $D_{10} \leq 10^{27}$ cm^2/s. Such a value of the diffusion coefficient is significantly smaller than the standard diffusion coefficient, $D_{10} \sim 10^{28}$ cm^2/s, which is commonly used for the galactic CR propagation models. Note however that for the models which assume the local origin of the observed cosmic rays [36,37], the smaller values of the diffusion coefficient (as low as 10^{26}–10^{27} cm^2/s) are preferable, in particular, in order to avoid a possible contradiction with the observed small CR anisotropy [37].

These estimates show that shock acceleration of electrons by a relatively young ($t \leq 10^5$ yr) and nearby ($r \sim 100$ pc) supernova remnant(s), like the Loops or the Geminga SNR, could easily explain the observed flux of high-energy electrons. However, this mechanism cannot explain the high content of positrons observed at $E \geq 10$ GeV. In fact, one may expect from SNR's also high-energy positrons of secondary origin produced at interactions of accelerated protons with ambient gas. However, as it is shown in [38], for conventional values of the total energy of accelerated protons $W_p \approx 10^{50}$ erg and gas density $n \approx 1$cm^{-3}, the flux of positrons provided by this mechanism cannot exceed 10% of the observed flux. Therefore, one must assume a more effective source of positrons. In [38] we discussed the possibility to attribute the observed flux of positrons to a nearby pulsar, for example Geminga. Thus, the high content of high-energy positrons in the electron flux leads to the conclusion that the nearby source should have a different origin than the bulk of sources (producing mainly negatrons) spread over the Galaxy and responsible for the G component. This rather strong (in fact, model-independent) conclusion implies a deviation of our local environment from the galactic "average" which is not straightforward, but cannot be excluded. Obviously, this statement needs further confirmation of the high positron flux. Future measurements will clarify the origin of the nearby source of TeV electrons.

---

[1] V. S. Berezinsky, S. V. Bulanov, V. L. Ginzburg, V. A. Dogiel, and V. S. Ptuskin, *Astrophysics of Cosmic Rays* (North-Holland, Amsterdam, 1990).

[2] C. J. Cesarsky, Annu. Rev. Astron. Astrophys. **18**, 289 (1980).

[3] D. Müller and K. Tang, in *Proceedings of the 21st International Cosmic Ray Conference*, Adelaide, Australia, 1989, edited by R. J. Protheroe (Graphic Services, Northfield, South Australia, 1990), Vol. 3, p. 249.

[4] M. Turner and F. Wilczek, Fermi National Accelerator Laboratory Report No. B9/44A, 1989 (unpublished).

[5] A. J. Tylka, Phys. Rev. Lett. **63**, 840 (1989).

[6] F. A. Aharonian and A. M. Atoyan, J. Phys. G **17**, 1769 (1991).

[7] C. S. Shen, Astrophys. J. **162**, L181 (1970).

[8] C. S. Shen and C. Y. Mao, Astrophys. Lett. **9**, 169 (1971).

[9] R. Cowsik and M. A. Lee, Astrophys. J. **228**, 297 (1979).

[10] J. Nishimura *et al.*, Astrophys. J. **238**, 394 (1980).

[11] T. Taira *et al.*, in *Cosmic Ray Conference*, Proceedings of the 23rd International Conference, Calgary, Canada, 1993, edited by R. Hicks, D. A. Leahy, and D. Venkatesan (World Scientific, Singapore, 1994), Vol. 2, p. 128.

[12] R. E. Lingenfelter, Nature (London) **224**, 1182 (1969).

[13] V. L. Ginzburg and S. I. Syrovatskii, *The Origin of Cosmic Rays* (Pergamon, Oxford, 1964).

[14] S. I. Syrovatskii, Sov. Astron. AJ **3**, 22 (1959).

[15] A. N. Tychonov and A. A. Samarskii, *Partial Differential Equations of Mathematical Physics* (Holden-Day, San Francisco, 1964).

[16] *Handbook of Mathematical Functions With Formulas, Graphs and Mathematical Tables*, edited by M. Abramowitz and I. A. Stegun (Dover, New York, 1968).

[17] G. R. Blumenthal and R. J. Gould, Rev. Mod. Phys. **42**, 237 (1970).

[18] G. Berkey and C. S. Shen, Phys. Rev. **188**, 1994 (1969).

[19] K. Tang, Astrophys. J. **278**, 881 (1984).

[20] R. L. Golden and B. G. Mauger, Astrophys. J. **287**, 622 (1984).
[21] G. Basini *et al.*, in *Proceedings of the 22nd International Cosmic Ray Conference*, Dublin, Ireland, 1991, edited by M. Cawley *et al.* (Dublin Institute for Advanced Studies, Dublin, 1992), Vol. 2, p. 137.
[22] W. R. Webber, G. A. Simpson, and H. V. Cane, Astrophys. J. **236**, 448 (1980).
[23] S. P. Swordy, D. Müller, P. Meyer, J. Heureux, and J. M. Grunsfeld, Astrophys. J. **349**, 625 (1990).
[24] J. L. Fanslow, R. C. Hartman, R. H. Hildebrand, and P. Meyer, Astrophys. J. **158**, 771 (1969).
[25] J. K. Daugherty, R. C. Hartman, and P. J. Schmidt, Astrophys. J. **198**, 493 (1975).
[26] A. Buffington, C. D. Orth, and G. F. Smooth, Astrophys. J. **199**, 699 (1975).
[27] D. Müller and K. Tang, Astrophys. J. **312**, 183 (1987).
[28] R. L. Golden *et al.*, Astron. Astrophys. **188**, 145 (1987).
[29] C. F. Kennel and F. V. Coroniti, Astrophys. J. **283**, 694 (1984).
[30] F. Pacini, Nature **216**, 567 (1967).
[31] H. E. Gunn and J. P. Ostriker, Nature **221**, 454 (1969).
[32] S. L. Shapiro and S. A. Teukolsky, *Black Holes, White Dwarfs, and Neutron Stars* (Wiley-Interscience, New York, 1983).
[33] M. Garcia-Munoz, J. A. Simpson, T. G. Guzik, J. P. Wefel, and S. H. Margolis, Astrophys. J. (Suppl.) **64**, 269 (1987).
[34] U. Heinbach and M. Simon (unpublished).
[35] D. Breitschwerdt, J. F. McKenzie, and H. J. Völk, Astron. Astrophys. **245**, 79 (1991).
[36] R. E. Streitmatter, V. K. Balasubrahmanyan, J. F. Ormes, and R. J. Protheroe, in *Proceedings of the 18th International Cosmic Ray Conference*, Bangalore, 1983, edited by N. Durgaprasad *et al.* (TIFR, Bombay, 1983), Vol. 2, p. 183.
[37] J. F. Ormes, in Ref. [36], Vol. 2, p. 187.
[38] F. A. Aharonian, A. M. Atoyan, and H. J. Völk, Astron. Astrophys. **294**, L41 (1995).